IOP Publishing Journal of Neural Engineering
J. Neural Eng. 12 (2015) 036006 (10pp) doi:10.1088/1741-2560/12/3/036006

Spatial decoupling of targets and flashing stimuli for visual brain–computer interfaces

Nicholas R Waytowich and Dean J Krusienski

Biomedical Engineering, Old Dominion University, Norfolk Virginia, USA

E-mail: nick.waytowich@gmail.com

Received 11 November 2014, revised 26 February 2015
Accepted for publication 27 February 2015
Published 15 April 2015

Abstract

Objective. Recently, paradigms using code-modulated visual evoked potentials (c-VEPs) have proven to achieve among the highest information transfer rates for noninvasive brain–computer interfaces (BCIs). One issue with current c-VEP paradigms, and visual-evoked paradigms in general, is that they require direct foveal fixation of the flashing stimuli. These interfaces are often visually unpleasant and can be irritating and fatiguing to the user, thus adversely impacting practical performance. In this study, a novel c-VEP BCI paradigm is presented that attempts to perform spatial decoupling of the targets and flashing stimuli using two distinct concepts: spatial separation and boundary positioning. *Approach.* For the paradigm, the flashing stimuli form a ring that encompasses the intended non-flashing targets, which are spatially separated from the stimuli. The user fixates on the desired target, which is classified using the changes to the EEG induced by the flashing stimuli located in the non-foveal visual field. Additionally, a subset of targets is also positioned at or near the stimulus boundaries, which decouples targets from direct association with a single stimulus. This allows a greater number of target locations for a fixed number of flashing stimuli. *Main results.* Results from 11 subjects showed practical classification accuracies for the non-foveal condition, with comparable performance to the direct-foveal condition for longer observation lengths. Online results from 5 subjects confirmed the offline results with an average accuracy across subjects of 95.6% for a 4-target condition. The offline analysis also indicated that targets positioned at or near the boundaries of two stimuli could be classified with the same accuracy as traditional superimposed (non-boundary) targets. *Significance.* The implications of this research are that c-VEPs can be detected and accurately classified to achieve comparable BCI performance without requiring potentially irritating direct foveation of flashing stimuli. Furthermore, this study shows that it is possible to increase the number of targets beyond the number of stimuli without degrading performance. Given the superior information transfer rate of c-VEP paradigms, these results can lead to the development of more practical and ergonomic BCIs.

Keywords: brain–computer interface, steady-state visual evoked potentials, code-modulated visual evoked potentials, electroencephalogram

(Some figures may appear in colour only in the online journal)

1. Introduction

Brain–computer interfaces (BCIs) are systems that directly decode brain activity to communicate user intent [1]. One of the most promising approaches for scalp electroencephalogram (EEG)-based BCIs utilizes flashing stimuli to elicit visual-evoked potentials (VEPs) over the occipital cortex. BCIs based on steady-state visual evoked potentials (SSVEPs) have been extensively studied and have proven to be among the most flexible and robust approaches [2]. The performance and reliability of SSVEP detection have been improved with advanced multichannel analysis techniques such as canonical correlation analysis (CCA) [3]. A variation known as the code-modulated VEP (c-VEP) [4] employs stimuli that flash according to binary, pseudo-random sequences known as *m*-sequences. Because *m*-sequences have

an autocorrelation of nearly zero for non-zero shifts of the sequence, each target can be flashed using distinct time-shifted versions of a single reference *m*-sequence. This eliminates potential steady-state stimulus frequency biases and allows for straightforward extension to larger numbers of targets compared to standard SSVEP. Thus, c-VEP paradigms have provided among the highest information transfer rates (ITRs) for noninvasive BCIs [5].

Visual irritation and fatigue from prolonged visual stimulation is an often overlooked issue that can significantly affect usability of VEP–BCIs in real-world scenarios [6, 7]. In the seminal study that yielded impressively high noninvasive BCI ITRs, Bin *et al* used a matrix of 32 targets that simultaneously flashed according to a time-shifted *m*-sequence [4]. The matrix was additionally encompassed by 28 complimentary flashing non-target stimuli for a total of 60 simultaneously flashing stimuli. Although this paradigm produced a comparatively high ITR for a noninvasive BCI, it generates a visual cacophony that is not visually pleasing or desirable for long-term use. Traditional solutions to this problem have been to reduce the saliency or obtrusiveness of the visual stimuli such as utilizing high-frequency stimulation (>35 Hz) [8, 9], high duty-cycle stimulation (<50% duty cycle) [10], or low-contrast stimulation (0–10% contrast) [11]. Although these approaches can reduce the reported visual fatigue, they generally compromise performance. For example, with the high-frequency stimulation, Muller *et al* [8] reported average accuracies near 69% with an average ITR of 46.8 bits min^{-1} with frequencies greater than 30 Hz, compared to average accuracies of 91% and an average ITR of 92.8 bits min^{-1} using c-VEP [12].

SSVEP BCIs that do not require direct foveation of the flashing stimuli have also been developed. These paradigms are ultimately designed for individuals who are unable to control their gaze, such as with locked-in syndrome [13]. Typically, these paradigms require the user to fixate their eye-gaze on a central, inactive position while focusing covert attention on a flashing target located in their parafoveal vision (i.e., $2 \simeq 5$ degrees of visual angle from foveal center [14]). While these paradigms achieve some degree of effectiveness, they generally suffer from a dramatic drop in performance compared to direct-gaze approaches, even when implementing a small number of targets [13, 15–17].

The present study proposes a novel c-VEP paradigm that incorporates two distinct concepts that spatially decouple the targets from the flashing stimuli. The first concept spatially separates the targets from the stimulus such that fixation of the target does not require direct foveation of the flashing stimuli, nor does it require covert attention. For the second concept, while traditional SSVEP and c-VEP paradigms generally require a unique stimulus per target location, the proposed paradigm allows for target locations associated with the boundaries of the stimuli. This effectively decouples the targets from association to a single stimulus and increases the number of possible targets for a fixed number of distinct stimuli.

To evaluate both of these concepts, the flashing stimuli form a ring that encompass the spatially separated non-flashing targets, i.e., the user's 'workspace'. Targets are also uniquely positioned at or near the boundaries of adjacent stimuli. The user attends to a non-flashing target and the non-foveal flashing stimuli modulate the EEG. Several target configurations are evaluated and compared to the traditional direct-foveal (i.e., superimposed) target approach using the same interface. The results indicate that comparable performance can be attained using the traditional direct-foveal and the proposed non-foveal approaches, and that boundary targets can be as effectively discriminated as traditional non-boundary targets. These findings provide important insights for the development of more ergonomic and practical visual flashing paradigms for BCIs.

2. Methodology

2.1. Experimental paradigm

The proposed paradigm utilizes c-VEP stimuli that form a circular ring encompassing the non-flashing targets as shown in figure 1. The ring is segmented into four distinct arcs that are each flashed according to time-shifted versions of a single *m*-sequence. An *m*-sequence length of 63 was selected for purposes of comparison to the results from Bin *et al* [4]. While a shorter *m*-sequence can be used for this four- stimulus configuration, the length 63 *m*-sequence was implemented to maintain the same stimulus interval and temporal dynamics as Bin's landmark study. Because there are only four stimuli in the present paradigm, the *m*-sequence was circularly shifted by 15 bit intervals (0.25 s) for each adjacent stimulus to minimize undesirable EEG correlations due to smaller temporal shifts. During flashing, the segments of the ring alternate between pure black and white according to the shifted *m*-sequence. The background is 50% gray tone.

Both offline and online experiments were conducted to evaluate the new paradigm. In the offline experiment, EEG data were collected during foveal fixation on 25 different target locations (see figure 1(a)) to test the effects of target position and distance from the stimuli on performance. Fixation crosses were placed in three concentric rings (eight crosses per ring) at varying radii from the center of the ring. Eight of the 25 targets were superimposed directly on the stimuli for direct comparison of traditional direct-foveal stimulation and parafoveal stimulation. Targets were also placed at or near the boundaries of adjacent stimuli to determine if the combination of these stimuli could create discriminable EEG patterns and effectively double the number of possible targets for a given number of stimuli.

2.1.1. Target location grouping. The stimulus-ring design allows for unique characterization of c-VEP stimulation by exploiting spatial asymmetries produced by the surrounding ring stimuli and the encompassed target locations. The targets shown in figure 1(a) can be grouped by location such that attending to a particular location will elicit either direct-foveal (<1 degree of visual angle from foveal center), near-foveal ($1 \simeq 2$ degrees of visual angle from foveal center), or

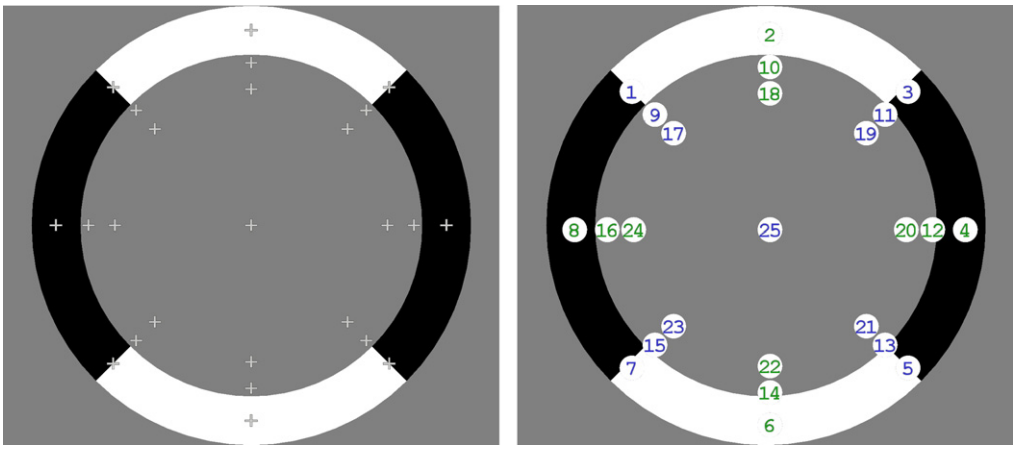

(a) (b)

Distance from Ring	Group #
Direct-Foveal	1) 8-Class (all)
(locations 1-8)	2) 4-Class (even)
Near-Foveal	3) 8-Class (all)
(locations 9-16)	4) 4-Class (even)
Parafoveal	5) 8-Class (all)
(locations 17-24)	6) 4-Class (even)

(c)

Figure 1. Workspace and target locations/groupings. (a) Four flashing c-VEP stimuli form a ring that encompass non-flashing targets indicated by the fixation crosses (+). During flashing, the segments of the ring alternate between pure black and white according to the shifted *m*-sequence. All 25 target locations used for offline evaluation are shown. Target locations are also placed directly over the stimuli to represent traditional direct-gaze stimulation. Only a single target is visible at any time for the offline experiments. (b) Target numbering for groupings. The odd numbers in blue represent the boundary targets and the even numbers in green represent the non-boundary targets. This numbering scheme is used to designate the concentric rings and the various 4- and 8-class classification configurations. (c) Target groupings for classification according to (b).

parafoveal ($2 \simeq 5$ degrees of visual angle from foveal center) visual stimulation. While there is no precise delineation of these foveal categorizations, the prescribed visual angles fall within the generally accepted ranges for foveal vision [14].

Additionally, targets can also be grouped as *boundary*, being on or adjacent to the boundary of two c-VEP stimuli; or *non-boundary*, on or adjacent to a single stimulus. As can be seen in figure 1(a), the targets that are in the boundary group lie on the diagonals of the ring and the non-boundary targets are on the horizontals and verticals of the ring. These boundary conditions were included to explore the effects of having two distinct and equally prominent stimuli representing the target, which has implications for increasing the number of possible target locations for a fixed number of flashing stimuli. The center target is equidistant from all ring stimuli and was included for comparison purposes, but was not included in the present analysis.

Based on this categorization scheme, several 8-target and 4-target classification groupings were considered, which are listed in figure 1(c). These 8- and 4-class configurations were used in the offline analysis to assess the quality of non-foveal c-VEP stimulation as a control signal for a BCI, as well as to explore the utility of the boundary targets in the 8-class configuration. While a wide variety of other groupings can be considered, particularly for offline analysis, the focus of the present study is to examine the effects of target distance from the stimuli and the impact of targets at or near the stimulus boundaries.

2.2. Data collection

A single experimental session was collected from twelve able-bodied subjects (five females, seven males, ages 21–28) for offline evaluation of the proposed paradigm. The subjects varied in previous BCI experience with seven subjects having no prior experience. This study was approved by Old Dominion University's Institutional Review Board and each subject gave informed consent before participating. Subjects reported no history of epilepsy or seizures, which can be induced in susceptible individuals by flashing stimuli. Data for one subject was excluded because the subject failed to comply with the task, and thus data from eleven subjects were analyzed. Five subjects (three females, two males) participated in a second session for an online evaluation of the proposed c-VEP paradigm in which real-time target selection feedback was provided.

For both the online and offline sessions, EEG was recorded using a 16-channel g.USBAmp amplifier and active electrodes (Guger Technologies, Austria) primarily placed

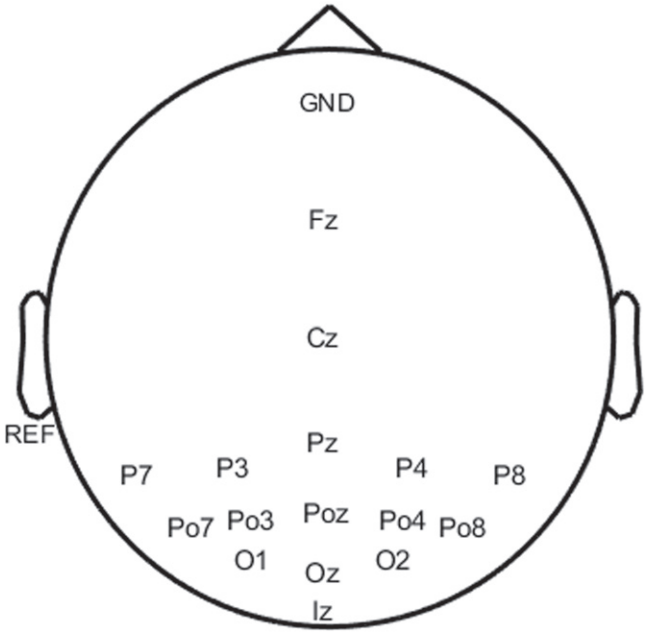

Figure 2. The EEG electrode montage used for the study. The locations are based on the international 10–20 system.

over the occipital and parietal-occipital regions of the brain as shown in figure 2. Signals were digitized at 600 Hz and stored on a hard disk. All EEG channels were referenced to the left ear-lobe and FPz was used as the ground. The EEG data recording was synchronized with the c-VEP task using UDP communication protocol with BCI2000 general-purpose BCI software [18].

Stimulus onsets for each *m*-sequence were synchronized using a digital trigger signal generated from an Arduino Mega microcontroller board with an Atmel ATmega1280 microcontroller that was connected to the recording computer. The *m*-sequence stimuli were displayed using DirectX (Microsoft Inc.). In both sessions, the c-VEP ring paradigm was displayed on a 40-inch LCD monitor with a refresh rate of 60 Hz.

Subjects sat in a darkened room in a comfortable chair, approximately 60 cm from the monitor. The stimulus ring subtended 45.2 H × 45.2W (radius = 50 cm) from the center. The parafoveal targets (locations 17–24) were centered 4.2 cm (4.0 degrees of visual angle) from the inner edge of the stimulus ring. The near-foveal targets (locations 9–16) were centered 1 cm (1.0 degree of visual angle) from the inner edge of the stimulus. The location of the subjects' gaze was recorded and verified using a TOBII X60 eye tracker, which was positioned directly below the monitor. The average radial standard deviation of the eye gaze for each target location and subject was computed to be 0.54 cm, which confirms that the subjects' gaze remained consistently fixated on the prescribed target locations.

2.2.1. Offline experiment. For the offline experiment, EEG data were collected for all 25 target locations. During the experiment, a single white fixation cross (i.e., target) was displayed at a time. Subjects were instructed to maintain visual fixation and attention on the cross during the stimulation period while refraining from unnecessary movements and frequent eye-blinks. Subjects attended to the target for 30 complete *m*-sequence cycles (31.5 s) while the segments of the ring simultaneously flashed with the respective lagged version of the *m*-sequence. After the 30-cycle stimulation interval, there was a 4 s pause while the target appeared in a new location and the process was repeated. Each of the 25 target locations were presented in random order to mitigate any anticipation and order biases. After 8 consecutive 30-cycle stimulation periods, a 1–2 min rest period was given. All 25 target locations were presented 4 times each totaling 126 s of data for each target location. The total session length for the offline experiment was approximately 1 h.

2.2.2. Online experiment. For the online experiment, two of the 4-class groups were used to evaluate the performance of the foveal and parafoveal target locations (groups 2 and 6, respectively, from the table in figure 1(c)). A training and testing session were conducted during a single larger session for 5 subjects that previously participated in the offline experiment. Only two 4-class conditions were evaluated online to keep the overall session length (training and testing) manageable in comparison to the prior offline session.

The training session was used to generate the c-VEP template waveforms for target identification. The training session was similar to the offline experiment except that only 8 total target locations were trained (the union of groups 2 and 6 as shown in the table in figure 1(c)). During training, only one target at a time was shown for 30 s with a 4 s blank interval. Presentation of each target position was again randomized. After completion of four repetitions of each of the 8 target locations, a custom Matlab script was used to generate the c-VEP templates as described in section 2.3.2. These templates were then utilized for classification during the online testing session. The online training session lasted approximately 25 min including rest periods.

Each of the 4-class conditions (i.e., foveal and parafoveal) was tested separately. During a trial, all four target locations from the particular condition were simultaneously displayed to the subject. A trial commenced with a 2 s cue period that indicated the intended target by highlighting it in blue as shown in figure 3(b). Next, EEG data were collected during a 6 s stimulation period. This was followed by a 2 s feedback period where target classification was performed and the predicted target was presented to the subject by highlighting the target in green as shown in figure 3(c). The ring stimuli started flashing 1 s into the cue period and remained flashing throughout the stimulation period. This was done to mitigate any transient ERP responses from the stimulus onset. The total trial (cue-stimulation-feedback) lasted 10 s. Figure 3(a) shows the timing protocol of a single online trial. After the feedback period, another trial commenced with a new target location. Sixteen trials constituted one run and two runs were performed for each 4-class condition. The online testing session lasted approximately 10 min, resulting in an overall online session

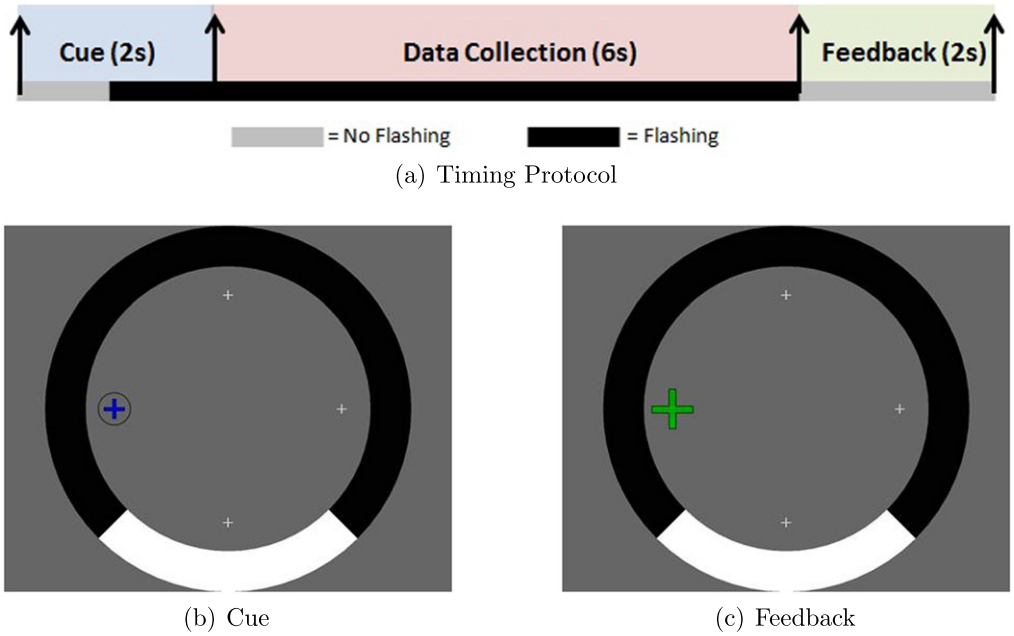

(a) Timing Protocol

(b) Cue (c) Feedback

Figure 3. (a) Timing protocol for an online trial. A two second cue segment highlights the target to attend to in blue (b). One second into the cue period, the ring stimuli started to flash. Data is collected for 6 s during the stimulation followed by a two second feedback period where the selected target is highlighted in green (c).

length of approximately 45 min including a 10 min interval for classifier calibration between the training and testing session.

2.2.3. Subjective evaluation. Following the online study, each subject was asked to subjectively evaluate the direct-foveal and the parafoveal conditions in terms of degree of visual irritation. For each condition, the subjects provided a numeric response to the following question: 'on a scale from 1–10, please rate how visually irritating it is to continuously stare at the target, with 1 representing not at all irritating and 10 representing extremely irritating'.

2.3. Data analysis

The analysis for this paradigm was based on Bin *et al* [4], in which CCA was adopted for multichannel c-VEP classification. Modifications to the method described in [4] were made such that the asymmetries of the ring paradigm could be exploited. Note that for the standard c-VEP BCI paradigm, which requires direct foveal fixation of the targets, the principle of equivalent neighbors [4] is employed and therefore only one target template needs to be constructed. In contrast, the various target locations in the present paradigm do not have equivalently positioned neighboring stimuli, so optimal spatial weights were computed using CCA for each target location.

2.3.1. Canonical correlation analysis. To reliably detect EEG responses to the flashing stimuli, a multivariate processing technique known as CCA can be utilized to find linear correlations between EEG data and a stimulating signal. CCA has recently been adopted for multidimensional EEG analysis and has proven to be extremely effective for SSVEP signal processing [3, 19]. CCA has also been extended for c-VEP classification [4].

CCA is a multi-dimensional correlation analysis technique that finds underlying correlations between two sets of data. It creates linear combinations of two multi-dimensional data sets such that the mutual projection between the two data sets is maximized. Given two multi-dimensional data sets X, and Y, and their respective linear combinations $x = X^T W_x$ and $y = Y^T W_y$, CCA determines the weight vectors W_x and W_y that produce the maximum correlation between x and y. The projected vectors x and y are known as canonical variants and their correlation is known as the canonical correlation. The weight vectors W_x and W_y that produce the highest canonical correlation are found by solving the optimization problem:

$$\max_{W_x, W_y} \rho(x, y) = \max_{W_x, W_y} \frac{E\left[W_x^T X Y^T W_y\right]}{\sqrt{E\left[W_x^T X X^T W_x\right] E\left[W_y^T Y Y^T W_y\right]}}. \quad (1)$$

In practice this can be solved using the singular-value decomposition method to diagonalize the covariance matrices as the maximum canonical correlation corresponds to the square-root of the largest eigenvalue.

2.3.2. Offline experiment. Data from the offline experiment were zero-phase band-passed filtered from 0.5–30 Hz using a Chebychev type II IIR filter, as 30 Hz is the largest frequency produced by a monitor with a 60 Hz refresh rate. All EEG channels were then re-referenced to channel Fz to eliminate potential hemispherical biases. Each 30-cycle stimulation trial

for each target location was extracted and concatenated to create 126 s (4 trials × 31.5 s) EEG segments for each target.

Data from each of the target groups listed in Table from figure 1(c) were aggregated, and target classification was performed to test the offline performance for each condition. For each condition, the 126 s data segments were separated into training and testing groups where 80% (96 cycles) was used for training and 20% (24 cycles) was used for testing. This ratio was selected because it gave sufficient training data to build the c-VEP templates for each target position. The c-VEP target templates, $M_k(t)$, were constructed using the training data by first averaging the multichannel EEG data, $X_k(t)$, across each m-sequence cycle to produce an averaged multichannel response, R_k, for each of the k target locations [4]. The resulting 1 s averaged responses were concatenated 100 times to produce a multichannel set S_k with the same dimensions as $X_k(t)$: $S_k = [R_k\, R_k\, R_k \ldots R_k\,]$.

CCA was then applied to find the best linear transformations of S_k and $X_k(t)$ that maximize the mutual projection, i.e., W_{S_k} and W_{X_k} such that $\rho(W_{X_k}^T X, W_{S_k}^T S)$ is maximized. The resulting W_{X_k} are spatial weights that are used to combine the multichannel templates to form the final template response for each target position. The testing data were then utilized to evaluate the target predictions for different observation lengths.

The test data for each target location were separated into trials (simulated observations) with integer cycle lengths from 1 cycle (1.05 s) to 6 cycles (6.3 s). The EEG for each trial was processed using the spatial weights W_{X_k} and classified for target prediction [4]. For a given observation of test data, the spatially filtered EEG was linearly correlated with each of the target templates from a given condition and the template with the maximum correlation was classified as the predicted target. The average of a 6-fold cross-validation scheme was used to determine the unbiased classification accuracy.

In order to assess the relative contribution of each channel to classification performance, a leave-one-out scheme was employed in which 14 of the 15 occipital channels were used in the classification [5]. The left-out channel was iterated through all channels. Left-out channels that resulted in a major drop in classification accuracy contributed more to the c-VEP response than left-out channels that resulted in little to no drop in accuracy. Because it was observed that excluding the worst performing channel generally boosted classification performance, the best 14 channels were selected for analysis. While CCA should theoretically assign an irrelevant channel a weight near zero, it is generally not identically zero, resulting in a noise component being added to the output of the spatial filter. Thus, an additional channel selection procedure may further boost CCA performance, particularly for larger channel sets. This simple channel exclusion procedure can be further optimized but is not expected to significantly affect the overall results of the present analysis.

2.3.3. Online experiment. The online experiment consisted of a training and testing session as part of a larger session. After the training data were collected, the c-VEP target templates for the target locations were constructed using the same procedure implemented in the offline experiment described in section 2.3.2. The CCA spatial weights for each template were also constructed. During the online test, a 2 s cue instructed the subject to attend to a particular target location, after which 6 s of data were collected during the stimulation period. The 6 s observations were classified as described in section 2.3.2 by filtering with W_{X_k}, correlating with each target template, and selecting the target with maximum correlation. As with the offline analysis, the simulated performance was evaluated for cycle lengths 1–5, where a cycle length of 6 represents the actual online performance. However, unlike the 4-class offline analysis, no cross-validation was performed to provide a more realistic estimate of actual online performance.

Table 1. Offline accuracies.

Distance from ring	Group #	Avg. accuracy
Direct-foveal (locations 1–8)	1) 8-class (all)	99.2% (±1.4)
	2) 4-class (even)	100% (±0.0)
Near-foveal (locations 9–16)	3) 8-class (all)	96.6% (±6.0)
	4) 4-class (even)	99.4% (±1.9)
Parafoveal (locations 17–24)	5) 8-class (all)	89.7% (±10.1)
	6) 4-class (even)	95.5% (±8.3)

3. Results

3.1. Offline experiment

The average accuracies for the offline experiment for each condition are shown in table 1. The accuracies are based on a 6-cycle observation length (6.3 s). The 8-class accuracies ranged from 89.7–99.2% and all of the 4-class conditions ranged from 95.5–100%. The average accuracies decreased with the distance from the target for all conditions. The 8-class parafoveal condition provided an average accuracy of 89.7% compared to 99.2% for the direct-foveal condition, which was statistically significant using a paired t-test ($p < 0.05$). The 4-class parafoveal condition provided an average accuracy of 95.5% compared to 100% for the direct-foveal condition, which was not statistically significant.

The two leftmost panels of figure 4 show the average offline performance as a function of the number of stimulus cycles used for classification for the 8- and 4-class conditions, respectively. In general, the performance monotonically increases with the number of stimulus cycles, but this creates a trade-off in terms of information transfer rate. For the 8-class condition, there was a statistically significant difference in accuracies between the foveal and parafoveal targets across all observation lenghts ($p < 0.05$ using a paired t-test). There was also a statistically significant difference between the near-foveal and parafoveal targets across all but the largest observation length. For the 4-class condition, there was a statistically significant difference in accuracy between the

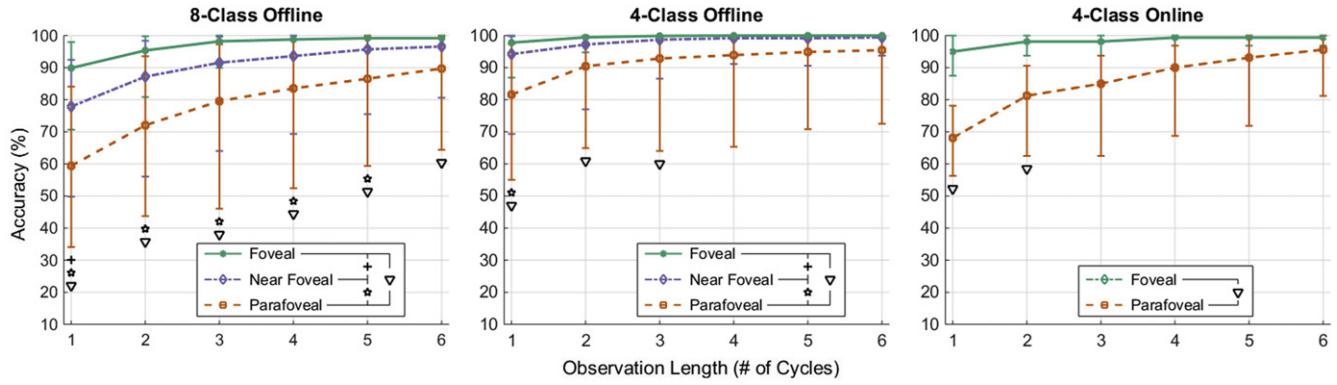

Figure 4. Simulated average classification accuracies for the offline and online experiments as a function of observation length in # of complete *m*-sequence cycles. The limits of the error bars indicate the minimum and maximum subject performance. A single *m*-sequence cycle length is 1.05 s, thus the observation lengths range from 1.05 s to 6.3 s. The markers in the legend indicate statistically significant differences ($p < 0.05$) between each condition at each observation length.

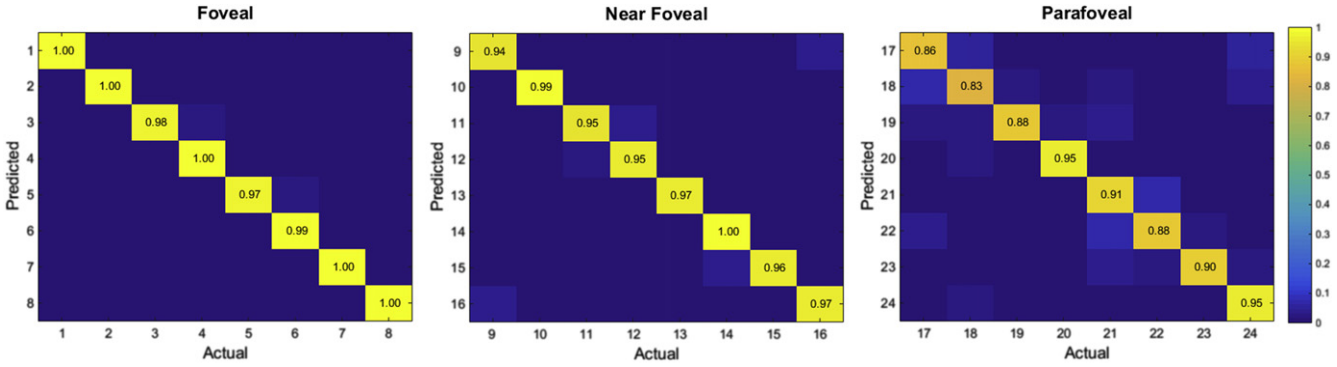

Figure 5. Confusion matrices for the three offline 8-class conditions (direct-foveal, near-foveal, parafoveal) for the 6.3 s observation length. The color scale indicates the proportion of classifications, with the diagonals labeled with the proportion of correct classifications. It is observed that there is no apparent bias in performance for the boundary target locations (odd numbers).

foveal and parafoveal targets only for the three shortest observation lengths.

In order to compare the relative classification performance of the targets at or near the boundaries of the stimuli, figure 5 shows confusion matrices for each of the 8-class conditions at the 6.3 s observation length. It is observed that there is no apparent bias in performance for the boundary target locations (odd numbers). Figure 6 shows the CCA spatial weight topographies and template waveforms for the foveal and parafoveal conditions, respectively, from a representative subject (S1).

3.2. Online experiment

The accuracies of the online experiment for the direct-foveal and parafoveal conditions are shown in table 2 for each subject. Both conditions provided average online accuracies of above 95%. The rightmost panel of figure 4 shows the simulated average performance as a function of the number of stimulus cycles used for the online data. Using a paired t-test, there was a statistically significant difference in accuracies between the conditions for the two shortest observation lengths ($p < 0.05$). Table 2 also includes the responses to the subjective evaluation of the perceived visual irritation on a scale from 1(least)-10(most), termed the irritation index.

4. Discussion

While existing VEP BCI paradigms almost exclusively prescribe visual targets that overlay or embody a single flashing visual stimulus, this study demonstrates the potential for spatially decoupling targets from individual flashing stimuli. The offline results for the 4-class condition in figure 4 indicate that there is no significant change in performance as the targets are positioned outside of direct foveal vision when an observation length greater than 4.2 s is used. The average performance across all conditions is above 80% after 3 (3.15 s) and 1 (1.05 s) stimulus cycles for the 8-class and 4-class scenarios, respectively. This indicates that the ring paradigm has the potential to achieve practical and competitive performance without requiring direct foveation of the targets.

Traditional VEP-BCIs generally associate a single target with a single, unique stimulus, which tends to create more visual discord for increasing numbers of targets. The proposed 8-class paradigm also introduces the novel concept of placing targets at or near the boundary of two adjacent stimuli. Figure 5 shows that there are no significant biases between the boundary and non-boundary classifications for a given condition. It can also be observed that

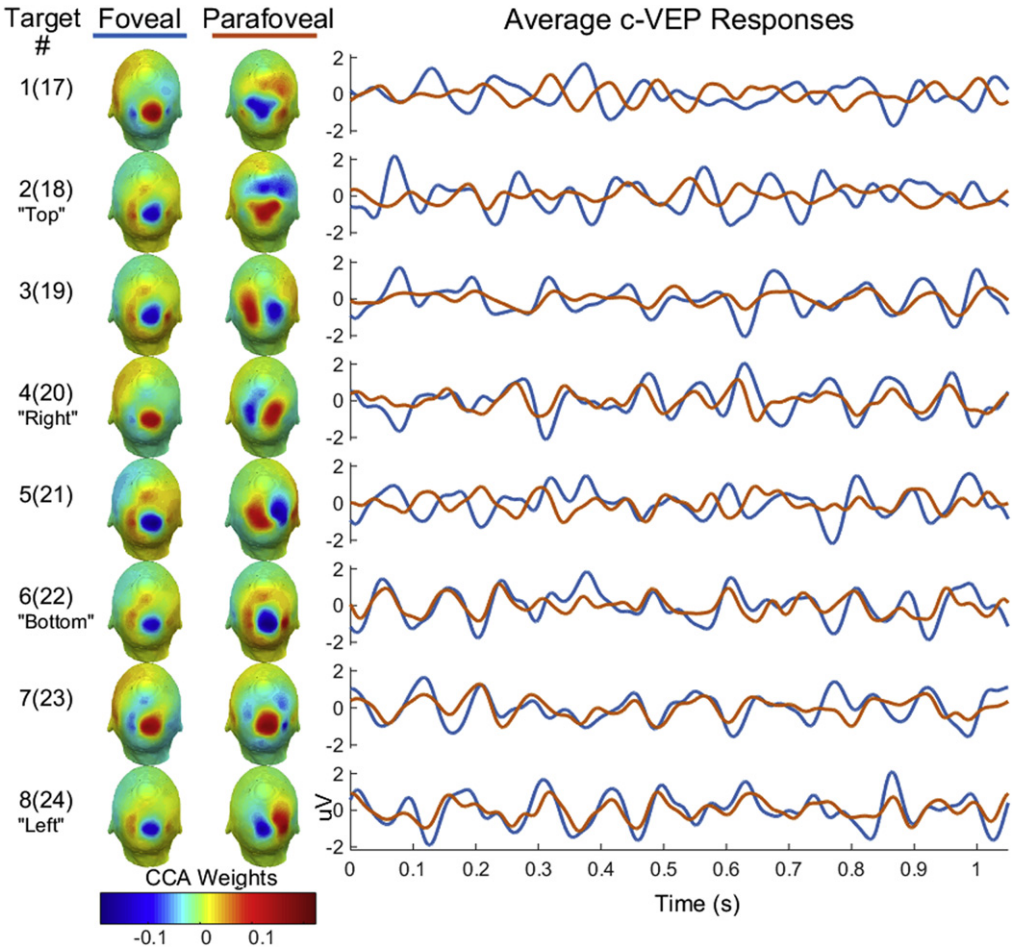

Figure 6. The CCA spatial weight topographies and template waveforms for the foveal and parafoveal conditions, respectively, from a representative subject (S1). The leftmost column indicates the spatially paired foveal(parafoveal) target numbers according to figure 1(b). The second and thrid columns show the CCA weight topographies for the foveal and parafoveal targets, respectively. The righmost column shows the CCA template wavforms for the foveal (blue) and parafoveal (red) targets.

Table 2. Online accuracies (t = 6.3 s) and visual irritation index.

	Foveal 4-class	Irritation index	Parafoveal 4-class	Irritation index
S1	100%	7	100%	5
S2	100%	8	100%	6
S9	96.9%	7	81.2%	3
S10	100%	8	96.9%	3
S11	100%	8	100%	5
Avg	**99.4%**	**7.6**	**95.6%**	**4.4**

misclassifications generally occur at adjacent targets along the diagonal, which is expected based on the design of the workspace.

The overall 8-class offline results demonstrate that it is possible to accurately detect and decode changes in the EEG due to multiple stimuli associated with a single target, although these results need to be verified using online experiments. While EEG changes due to multiple non-foveal stimuli have been utilized in the past, particularly with the principle of equivalent neighbors from the c-VEP speller introduced by Bin *et al* [4], the present study utilizes stimuli in a unique way such that there are more available targets than stimuli. This may help to mitigate the limits on the number of available traditional stimuli/targets imposed by the length of the *m*-sequence, monitor refresh rate, etc. Additionally, minimizing the number of required flashing stimuli may also have implications in terms of visual irritation and fatigue, although visual fatigue was not directly assessed in this study. Further investigations can be conducted to explore the effects of stimulus size, proximity, orientation, multiple boundaries, etc on performance.

The CCA template waveforms presented in figure 6 indicate that there is not a clear visual relationship between the foveal and parafoveal response templates. While the foveal and parafoveal templates for some corresponding target locations appear highly correlated (e.g., the bottom targets), others do not appear to have a distinct temporal relationship (e.g., the top targets). This is in contrast to Bin *et al* (2011), where the responses for each target were consistent due to the principle of equivalent neighbors (i.e., each target had identical boundary stimulus configurations and timing) [4]. Related to this point, it is not obvious how the adjacent stimuli contribute to the boundary target responses.

Again, each boundary stimulus has a different spatial orientation and further analysis is needed to quantify the relative contributions. Consistent with the differences in the CCA response templates, the CCA spatial weight topographies are similar between the foveal and parafoveal conditions for certain target locations (e.g., bottom) and dissimilar for other locations (e.g., top). The spatial weights with the largest magnitudes are generally focused over the central-occipital area for the foveal condition and more diffuse around the central-occipital area for the parafoveal condition, which is indicative of the contribution of peripheral vision. Similarities between adjacent patterns may provide some indication of the relative contributions of the adjacent stimuli to the boundary targets. These patterns were generally similar for the other subjects, but due to subtle differences between subjects, the patterns are most distinct when visualizing a single subject's data compared to a grand average across subjects.

The 4-class online results show more of a deviation in performance between the conditions for shorter observation lengths compared to the equivalent offline condition. This can be partially attributed to the comparatively lower performance of subject 9 for the parafoveal condition and that fewer subjects are represented in the average compared to the offline results. However, there is also a discrepancy in the relative performance ranges between the online and offline results, particularly for the parafoveal condition. One likely explanation is that the stimulus duration for the offline data was longer and the cross-validation procedure included segments of training data that did not begin from the stimulus onset and were from the middle of the trials. Therefore, it is likely that the simulated observations from the middle of the offline trials are fully entrained to the stimuli and do not include any transient effects of the stimulus onset. Thus, this offline training data is more representative of the entrained EEG of the later cycles and misleadingly indicates better performance compared to the online condition where the EEG of the early cycles may not be fully entrained. Nevertheless, the online parafoveal condition still attains an average accuracy above 80% after 2 (2.1 s) stimulus cycles. This may provide a favorable trade-off between performance and visual irritation since the online subjects universally rated the parafoveal condition as less irritating as indicated in table 2.

In order to fully validate the paradigm, undirected free-choice online experiments should be conducted to account for practical use issues such as target scanning and reaction to task-related feedback. Future work will more thoroughly explore the effects of distance between the targets and stimuli, increasing the number of stimuli/boundaries along the ring, the use of shorter *m*-sequences, and larger N-class target configurations that further exploit the combined concepts of stimulus-target distance and boundaries. It is envisioned that these stimulus-target decoupling concepts introduced in the proposed paradigm will lead to the development of more practical and ergonomic BCIs by reducing visual irritation and potentially fatigue, as well as by increasing the number of available targets for a fixed number of stimuli.

Acknowledgments

This work was supported by the National Science Foundation Division of Information and Intelligent Systems (1064912).

References

[1] Wolpaw J R, Birbaumer N, McFarland D J, Pfurtscheller G and Vaughan T M 2002 Brain–computer interfaces for communication and control *Clin. Neurophysiol.: Official J. Int. Fed. Clin. Neurophysiol.* **113** 767–91

[2] Middendorf M, McMillan G, Calhoun G and Jones K S 2000 Brain–computer interfaces based on the steady-state visual-evoked response. *IEEE Trans. Rehabil. Eng. : Publ. IEEE Eng. Med. Biol. Soc.* **8** 211–4

[3] Bin G, Gao X, Yan Z, Hong B and Gao S 2009 An online multi-channel SSVEP-based brain–computer interface using a canonical correlation analysis method *J. Neural Eng.* **6** 046002

[4] Bin G, Gao X, Wang Y, Li Y, Hong B and Gao S 2011 A high-speed BCI based on code modulation VEP *J Neural Eng.* **8** 025015

[5] Spüler M, Rosenstiel W and Bogdan M 2012 Online adaptation of a c-VEP brain–computer interface (BCI) based on error-related potentials and unsupervised learning *PloS One* **7** e51077

[6] Boksem M a S, Meijman T F and Lorist M M 2005 Effects of mental fatigue on attention: an ERP study *Brain Res. Cogn. Brain Res.* **25** 107–16

[7] Hong B, Guo F, Liu T, Gao X and Gao S 2009 N200-speller using motion-onset visual response *Clin. Neurophysiol.: Official J. Int. Fed. Clin. Neurophysiol.* **120** 1658–66

[8] Müller S M T, Diez P F, Bastos-Filho T F, Sarcinelli-Filho M, Mut V and Laciar E 2011 SSVEP–BCI implementation for 37–40 Hz frequency range *Annual Int. Conf. IEEE Engineering in Medicine and Biology Society* **2011** 6352–5

[9] Diez P F, Torres Müller S M, Mut V A, Laciar E, Avila E, Bastos-Filho T F and Sarcinelli-Filho M 2013 Commanding a robotic wheelchair with a high-frequency steady-state visual evoked potential based brain–computer interface *Med. Eng. Phys.* **35** 1155–64

[10] Lee P-L, Yeh C-L, Cheng J Y-S, Yang C-Y and Lan G-Y 2011 An SSVEP-based BCI using high duty-cycle visual flicker *IEEE Trans. Biomed. Eng.* **58** 3350–9

[11] Lalor E C and Foxe J J 2009 Visual evoked spread spectrum analysis (VESPA) responses to stimuli biased towards magnocellular and parvocellular pathways *Vis. Res.* **49** 127–33

[12] Bin G, Gao X, Wang Y and Hong B 2009 VEP-based brain–computer interfaces: time, frequency, and code modulations *Computational Intelligence* **4** 22–6

[13] Lesenfants D *et al* 2014 An independent ssvep-based brain–computer interface in locked-in syndrome *J. Neural Eng.* **11** 035002

[14] Westheimer G 1982 The spatial grain of the perifoveal visual field *Vis. Res.* 157–62

[15] Allison B Z, McFarland D J, Schalk G, Zheng S D, Jackson M M and Wolpaw J R 2008 Towards an independent brain–computer interface using steady state

visual evoked potentials *Clin. Neurophysiol.: Official J. Int. Fed. Clin. Neurophysiol.* **119** 399–408

[16] Lalor E C, Kelly S P, Pearlmutter B a, Reilly R B and Foxe J J 2007 Isolating endogenous visuo-spatial attentional effects using the novel visual-evoked spread spectrum analysis (VESPA) technique *Eur. J. Neurosci.* **26** 3536–42

[17] Kelly S P, Lalor E, Finucane C and Reilly R B 2004 A comparison of covert and overt attention as a control option in a steady-state visual evoked potential-based brain–computer interface *Annual Int. Conf. IEEE Engineering in Medicine and Biology Society* **7** 4725–8

[18] Schalk G, McFarland D J, Hinterberger T, Birbaumer N and Wolpaw J R 2004 Bci2000: a general-purpose brain–computer interface (bci) system *IEEE Trans. Biomed. Eng.* **51** 1034–43

[19] Lin Z, Zhang C, Wu W and Gao X 2007 Frequency recognition based on canonical correlation analysis for SSVEP-based BCIs *IEEE Trans. Biomed. Eng.* **54** 1172–6